

The Effect of Single Crystalline Substrates and Ion-Beam Bombardment on Exchange Bias in Nanocrystalline NiO/Ni₈₀Fe₂₀ Bilayers

D. L. Cortie^{1,2}, C. Shueh³, B.-C. Lai³, P. W. T. Pong⁴, J. van Lierop⁵, F. Klose², and K.-W. Lin³

¹Institute for Superconducting and Electronic Materials, University of Wollongong, NSW, Australia

²Australian Nuclear Science and Technology Organisation, NSW, Australia

³Department of Materials Science and Engineering, National Chung Hsing University, Taichung 402, Taiwan

⁴Department of Electrical and Electronic Engineering, The University of Hong Kong, Hong Kong

⁵Department of Physics and Astronomy, University of Manitoba, Winnipeg, R3T 2N2, Canada

Methods to modify the magnetic coercivity and exchange bias field of nanocrystalline antiferromagnetic/ferromagnetic NiO/Ni₈₀Fe₂₀ thin films were investigated for bilayers grown using ion-assisted deposition onto different single crystalline substrates. An enhanced coercivity was found at 298 K for the films deposited on single crystalline MgO (100) and Al₂O₃ (11-20) substrates. After field cooling the films to 50 K, the NiO/NiFe bilayer grown on Al₂O₃ (11-20) exhibited the largest exchange bias (-25 Oe). The second part of the study investigated ion-beam modification of the ferromagnetic surface prior to the deposition of the NiO layer. A range of ion-beam bombardment energies (V_{EH}) were used to modify *in situ* the NiFe surface during the deposition of NiO/NiFe/SiO₂ films. Cross-sectional transmission electron microscopy showed a systematic reduction in the thickness of the NiFe layers with increasing Ar⁺ bombardment energies attributed to etching of the surface. In addition, the bombardment procedure modified the magnetic exchange bias of the composite structure in both the as-prepared and field-cooled state.

Index Terms—Exchange bias, ion-beam modification.

I. INTRODUCTION

THE insulating antiferromagnet oxide materials such as NiO ($T_N \sim 523$ K) and α -Fe₂O₃ ($T_N \sim 925$ K) have high magnetic ordering temperatures in their bulk forms and are corrosion resistant [1]. These two important properties motivated past investigations into using these materials for exchange bias systems and spin-valves to operate above room temperature [2], [3]. Such devices aim to exploit the interfacial coupling of antiferromagnetic order to a neighboring ferromagnet, in order to generate a shifted hysteresis loop. The precise control and understanding of this exchange bias shift using antiferromagnet oxides has become an increasingly important topic for the next-generation of devices [4], [5]. However, past studies of exchange bias systems that used NiO generally found the thermal stability, thermal conductivity and blocking temperature to be less suitable than that of metallic counterparts such as IrMn₃, and oxide materials are not widely employed in the contemporary magnetic storage industry [6]. For example, some studies have reported a notable exchange bias at room temperature using NiO with a blocking temperature of ~ 450 K [7], [8], whereas other studies have reported blocking temperatures beneath room temperature [9]. A previous study reported a room temperature exchange bias field that depended inversely on the mean-grain size of the NiO layer [7], in accordance with Takano's model for the similar face-centered-cubic (fcc) oxide CoO [10]. However, according to studies, small grains may present thermal instability (e.g., superparamagnetism assuming a thermal fluctuation description) at higher temperatures, therefore breaking the rule of

inverse scaling with antiferromagnet grain size [8], [11]. It is also clear that other microstructural features such as interface mixing [9], nonmagnetic defects [12], preferred crystallite orientation [13] and layer thickness [14] can play the decisive role in the magnitude and temperature dependency of exchange bias. Owing to this rich complexity, methods such as epitaxial growth and *in situ* surface-modification of nanocrystalline NiO/NiFe bilayers using ions are helpful to establish trends [15]. In past work, the effect of ion-beam modification of the NiO interface layer in NiO/NiFe systems was studied [9], [16]. In the current work, the deposition sequence of the bilayer was reversed from NiFe/NiO/substrate to NiO/NiFe/substrate. A systematic study was performed on the resulting NiO/NiFe films grown by ion-assisted deposition to understand the effect of different crystalline substrates, and of exposing the ferromagnetic NiFe surface to different ion-bombardment steps prior to the deposition of the NiO layer. This paper is organized in the following way: Section II discusses the deposition and characterization procedure, Section III discusses the effects of the various substrates studied and Section IV discusses the effects of the ion-beam bombardment.

II. EXPERIMENTAL METHODS

A dual ion-beam deposition technique [16] was used to prepare the NiO/NiFe bilayers on the following substrates: amorphous SiO₂, single crystalline MgO [(100), (110) and (111)] and Al₂O₃ [(0001) and (11-20)]. The deposition was performed at room temperature in all cases. A Kaufman source was used to focus an argon ion-beam onto a commercial Ni₈₀Fe₂₀ (at %) or Ni target surface. An End-Hall source was used to *in situ* bombard the substrate for cleaning, or, during deposition using the Ni target, deposit the NiO layers (with a 16%O₂/Ar mixture from the source). For the NiO(~ 20 nm)/NiFe (~ 80 nm) films presented in Section III, a 150 Oe field was applied during deposition. For the NiO(~ 35 nm)/NiFe (~ 18 nm) films presented

Manuscript received May 05, 2013; revised July 12, 2013; accepted July 19, 2013. Date of current version December 23, 2013. Corresponding author: K.-W. Lin (e-mail: kwlin@dragon.nchu.edu.tw).

Color versions of one or more of the figures in this paper are available online at <http://ieeexplore.ieee.org>.

Digital Object Identifier 10.1109/TMAG.2013.2274654

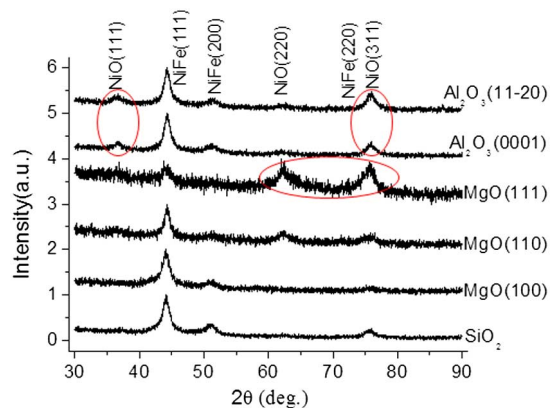


Fig. 1 XRD patterns for the NiO (20 nm)/NiFe (80 nm) bilayers deposited on different substrates under otherwise identical conditions.

in Section IV, no field was applied during deposition, however the surfaces of the bottom NiFe layers were bombarded with different Ar ion-beam energies ($V_{EH} = 0-150$ V) for 5 minutes before the bilayer was completed via capping with 35 nm of NiO. The crystal structures of the NiO/NiFe bilayers were characterized using grazing incidence X-ray diffraction (GI-XRD) using a Bruker AXS diffractometer. A JEOL (JEM-2010) transmission electron microscope (TEM) operating at 200 kV was used for microstructural analysis. Magnetic measurements were performed in a Quantum Design VSM or MPMS. External fields were always applied in the in-plane direction. In these measurements, the exchange bias (H_{EB}) is measured from the shift of the hysteresis loop: $H_{EB} = (H_{c1} + H_{c2})/2$ where H_{c1} and H_{c2} are the negative and positive field region coercivities, respectively. In each case, the results are given for the virgin loop (i.e., in the untrained state).

III. RESULTS AND DISCUSSION

Fig. 1 shows the X-ray diffraction (XRD) patterns collected in grazing angle incidence geometry for the six NiFe/NiO samples deposited on different substrates under otherwise identical external conditions. In all cases, the lattice constants of the fcc NiFe and NiO are found to be 3.55 Å and 4.16 Å respectively. It appears that the choice of substrate did not alter the lattice constant of the films greatly, but only modified subtly the film texture/orientation. Fig. 2(a) shows the high resolution cross-sectional TEM image of the bilayer on the SiO₂ substrate. The nominal thickness of the two layers is 20 nm for the NiO layer and 80 nm for NiFe layer. Fig. 2(b) presents the plane-view TEM image in bright field and dark field and shows that both the NiFe and NiO are nanostructured with a grain size in the 5-10 nm range. Fig. 2(c) shows the selected area electron diffraction pattern of the NiO(~ 20 nm)/NiFe(~ 80 nm) bilayer on SiO₂. The spherically symmetric diffraction pattern can be indexed by assuming an isotropic orientation of fcc NiO and NiFe grains.

Fig. 3 presents the magnetic hysteresis loops for the six samples on the different substrates at 298 K. In all cases, the coercivity was found to be less than 10 Oe, however the samples prepared on MgO (111), MgO(100) and Al₂O₃ (11-20) have moderately higher coercive field values ($H_c = 8, 8,$ and 7 Oe, re-

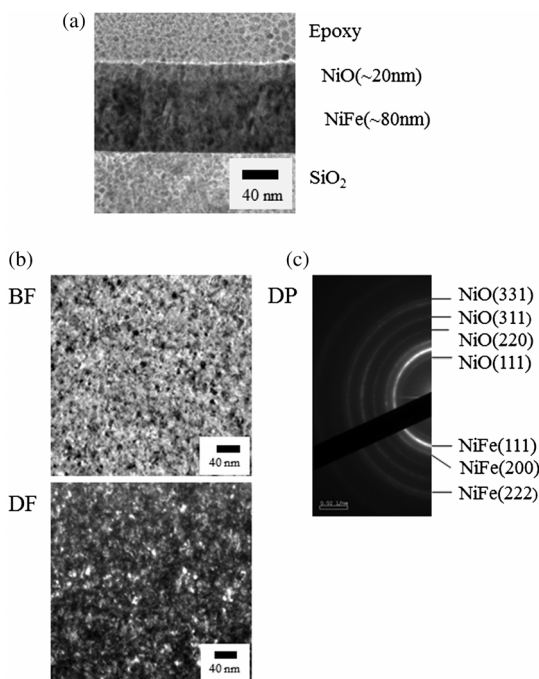


Fig. 2 (a) High resolution cross-sectional TEM image of a NiO(20 nm)/NiFe(80 nm) film on a SiO₂ substrate showing a clear bilayer structure and sharp interface. (b) Plane view bright field (BF) and dark field (DF) TEM images of the same sample. (c) Selected area electron diffraction pattern (SAED) showing a polycrystalline and random orientation of NiO grains.

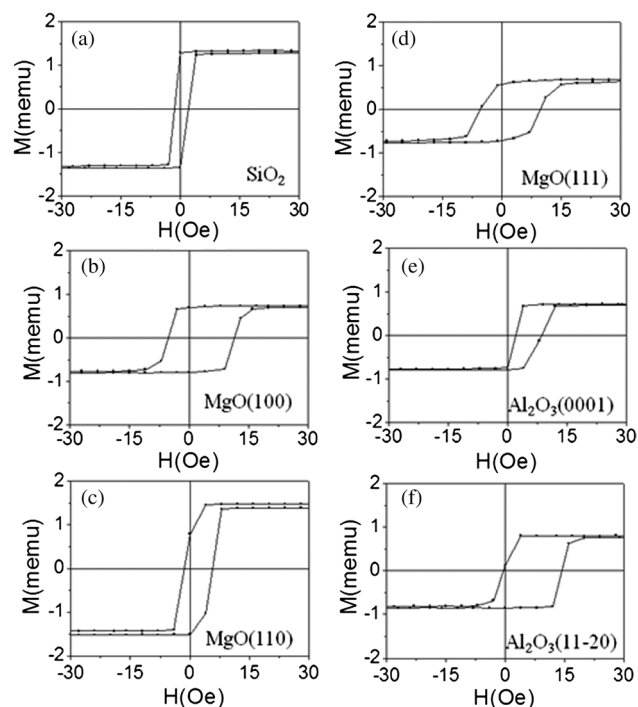


Fig. 3 Magnetic hysteresis loops at 298 K for the NiO(~ 20 nm)/NiFe(~ 80 nm) bilayers deposited on different substrates as discussed in the text.

spectively) than those deposited in SiO₂ ($H_c \sim 2$ Oe). In all cases, low exchange bias (< 5 Oe) is found at 298 K, despite the application of the 150 Oe field during deposition. Fig. 4 shows the hysteresis loops of the same samples upon field cooling in 12 kOe from 298 to 50 K. The maximum exchange bias is seen for the Al₂O₃ (11-20) ($|H_{EB}| \sim 11$ Oe) and MgO

TABLE I
COMPARISON OF EXCHANGE BIAS OF BOMBARDED AND UNBOMBARDED NiO/NiFe BILAYERS ON VARIOUS SUBSTRATES¹

Substrate[Ar ⁺ bombardment energy]	Nominal layer thickness (nm)	H _{EB} (Oe) at 298 K	H _C (Oe) at 298K	H _{EB} (Oe) after field cooling	H _C (Oe) after field cooling
MgO 110 [none]	NiFe 80 NiO 20	0	4	1*	5*
MgO 100 [none]	NiFe 80 NiO 20	1	8	5*	10*
MgO 111 [none]	NiFe 80 NiO 20	0	8	1*	8*
Al ₂ O ₃ (0001) [none]	NiFe 80 NiO 20	3	3	2*	15*
Al ₂ O ₃ (11-20) [none]	NiFe 80 NiO 20	5	7	11*	26*
SiO ₂ [V _{EH} = 0 V]	NiFe 18 NiO 35	7	4	86	150
SiO ₂ [V _{EH} = 70 V]	NiFe 15 NiO 35	31	4	52	90
SiO ₂ [V _{EH} = 100 V]	NiFe 13 NiO 35	0	7	22	96
SiO ₂ [V _{EH} = 130 V]	NiFe 7 NiO 35	40	10	38	190

¹ Samples marked with an asterisk in Table I were field cooled to from 298 K to 50 K in 12 kOe field whereas those without an asterisk were field cooled from 298 K to 5 K in 20 kOe.

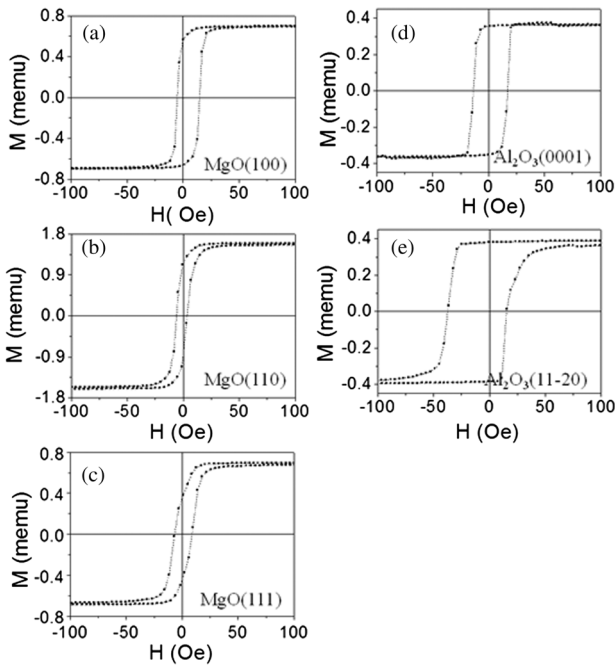


Fig. 4 Magnetic hysteresis loops at 50 K for the NiO(20 nm)/NiFe(80 nm) bilayer deposited on different substrates, after in-plane field cooling from 298 K to 50 K in 12 kOe.

(100) substrate ($|H_{EB}| \sim 5$ Oe). In the other cases, the exchange bias values remain low and near the remnant field due to trapped flux in the magnetometer's superconducting solenoid (e.g. 2-4 Oe). Therefore, it appears that in general, the exchange bias is low for the nanocrystalline samples studied here in this thickness regime, although the film structure shows some dependence on the underlying substrate. The various values of exchange bias and coercive fields on different substrates are collected in Table I.

IV. EFFECT OF ION-BOMBARDMENT

Fig. 5 shows the high resolution cross-sectional TEM images for NiO(35 or 5 nm)/NiFe(x nm) films on SiO₂ where the initial 18 nm NiFe layer was subjected to Ar⁺ ion-bombardment at energies in the range $V_{EH} = 0$ -130 V prior to deposition of the NiO. For comparison, samples with two thickness of

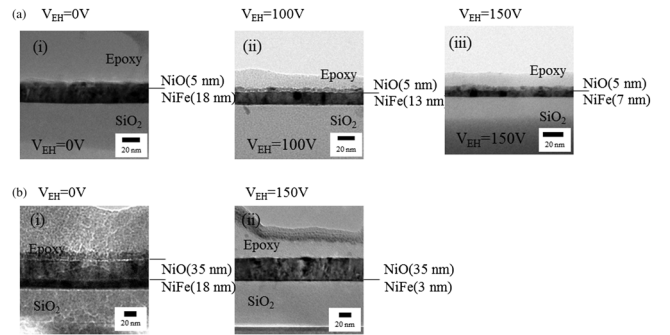


Fig. 5 High resolution cross-sectional TEM image of (top a) NiFe(x nm)/NiO(5 nm) and (lower b) NiO(30 nm)/NiFe(x nm) bilayers on SiO₂ where the NiFe surface was *in situ* bombarded with Ar⁺ ions at various energies (V_{EH}) for 5 minutes prior to capping with NiO.

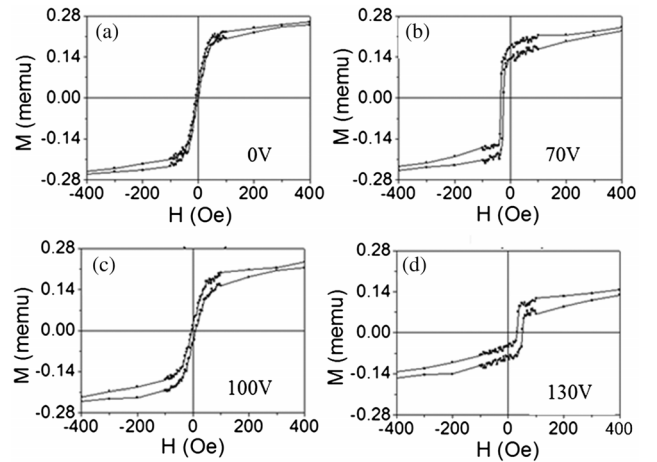


Fig. 6 Magnetic hysteresis loops at 298 K for the NiO(35 nm)/NiFe(x nm) bilayers on SiO₂ where the NiFe surface was *in situ* bombarded with Ar⁺ ions at various energies (V_{EH}) for 5 minutes prior to capping with NiO.

NiO (35 and 5 nm) are shown. The thickness of the NiFe layer is reduced systematically with increasing ion-bombardment energy. Fig. 6 shows the room temperature hysteresis loop of the NiO(35 nm)/NiFe(x nm) series illustrating a clear dependence of the magnetic properties on the ion-bombardment energy (V_{EH}). Despite the absence of a deposition field or a field cooling step, a significant exchange bias was found at

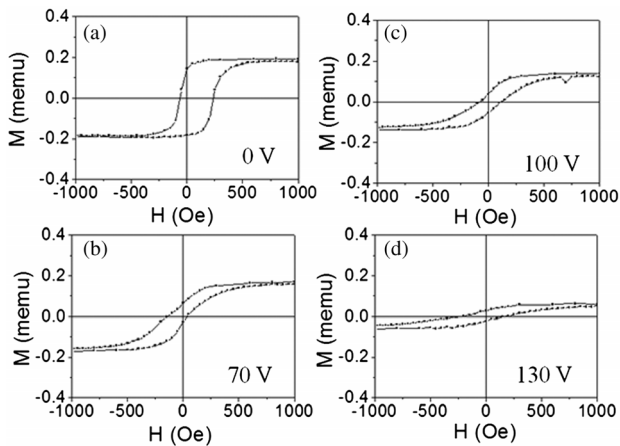


Fig. 7 Magnetic hysteresis loops at 5 K after in-plane field cooling from 298 K to 5 K in 20 kOe for the NiO(35 nm)/NiFe(x nm) bilayers on SiO₂ where the NiFe surface was *in situ* bombarded with Ar⁺ ions at various energies (V_{EH}) for 5 minutes prior to capping with NiO.

298 K, which depended on the ion-beam bombardment energy (V_{EH}). The exchange bias field had a maximum magnitude for the samples with $V_{EH} = 70$ V ($|H_{EB}| \sim 30$ Oe) and $V_{EH} = 130$ V ($|H_{EB}| \sim 40$ Oe). As no field cooling step was applied, the modifications observed in exchange bias sign may be consistent with variable anisotropy directions in the as-prepared state. Note that only the results for the NiO (35 nm) films are discussed since no exchange bias was found for the NiO (5 nm) films, which agrees with a recent result that the critical thickness for exchange bias with a NiO layer is > 15 nm [14]. Fig. 7 shows the low temperature hysteresis loops for the NiO(35 nm)/NiFe(x nm) films after field cooling. In all cases the coercive field values are increased from < 10 Oe at 298 K to ~ 90 -190 Oe at 5 K, indicating the increased strength of the interfacial exchange. Overall, the range of exchange bias values increased to 20–80 Oe at 5 K. However, it appears that the sample $V_{EH} = 0$ which has a low H_{EB} at 298 K, possesses the highest exchange bias at low temperature. Collectively, these findings suggest that ion-beam bombardment has a complex effect on the magnitude and the temperature dependency of exchange bias.

V. CONCLUSION

The magnetometry results are summarized for the various samples in Table I. Our previous work has shown that ion-beam bombardment of the NiO surface may create uncompensated antiferromagnetic moments giving rise to an enhanced exchange bias field at 5 K [16]. However, in this work, we found that increased bombardment of the Ni₈₀Fe₂₀ surface generally resulted in a smaller magnitude of exchange bias at 5 K. This suggests that the ion-beam modification had a different effect, likely the introduction of defects at the ferromagnetic surface. Careful analysis will be needed to assess the origin of the effects of the ion-beam bombardment. It is clear from the experiments that

a change in sign of the exchange bias is observed using identical field cooling conditions depending on the ion-beam bombardment energy. Conventionally, reversal in the exchange bias polarity has been attributed to a change in the sign of interface coupling from ferromagnetic to antiferromagnet, in addition to a sufficiently high cooling field [17]. In the present case, the origin of this oscillating behavior requires further investigations since field cooling from below the blocking temperature with an unknown anisotropy direction could give similar results. Regardless, this behavior is only seen in the ion-beam bombarded samples. Future work is required to control the deposition and bombardment conditions to result in constant thickness films and use high temperature field cooling procedures to controllably set the interfacial spin alignment during the antiferromagnet's magnetic ordering transition (e.g., T_N).

ACKNOWLEDGMENT

This work was supported by the NSC of Taiwan and NSERC of Canada. The work of D. Cortie was supported by the Australian Institute of Nuclear Science and Engineering.

REFERENCES

- [1] C. N. R. Rao and B. Raveau, *Transition Metal Oxides: Structure, Properties and Synthesis of Ceramic Oxides*. New York, NY, USA: Wiley, 1998.
- [2] Y. Hamakawa *et al.*, "Spin-valve head utilizing antiferromagnetic NiO layers," *IEEE Trans. Magn.*, vol. 32, no. 1, p. 149, Jan. 1996.
- [3] M. Pinarbasi *et al.*, "Antiparallel pinned NiO spin valve sensor for GMR head application," *J. Appl. Phys.*, vol. 87, p. 5714, 2000.
- [4] X. He *et al.*, "Robust isothermal electric control of exchange bias at room temperature," *Nature. Mat.*, vol. 9, p. 579, 2010.
- [5] Y.-H. Chu *et al.*, "Electric-field control of local ferromagnetism using a magnetoelectric multiferroic," *Nature Mat.*, vol. 7, p. 478, 2008.
- [6] K. O'Grady *et al.*, "A new paradigm for exchange bias in polycrystalline thin films," *J. Magn. Magn. Mater.*, vol. 322, p. 883, 2010.
- [7] C.-H. Nam *et al.*, "Dependence of exchange coupling on NiO grain size in NiO/NiFe bilayers," *J. Appl. Phys.*, vol. 93, p. 6584, 2003.
- [8] A. F. Khapikov *et al.*, "Temperature dependence of exchange field and coercivity in polycrystalline NiO/NiFe film with thin antiferromagnetic layer: Role of antiferromagnet grain size distribution," *J. Appl. Phys.*, vol. 87, p. 4954, 2000.
- [9] K.-W. Lin *et al.*, "Tailoring interfacial exchange coupling with low-energy ion beam bombardment: Tuning the interface roughness," *App. Phys. Lett.*, vol. 100, p. 122409, 2012.
- [10] K. Takano *et al.*, "Interfacial uncompensated antiferromagnetic spins: Role in unidirectional anisotropy in polycrystalline Ni₈₁Fe₁₉/CoO bilayers," *Phys. Rev. Lett.*, vol. 79, p. 1130, 1997.
- [11] E. Fulcomer and S. H. Charap, "Thermal fluctuation aftereffect model for some systems with ferromagnetic-antiferromagnetic coupling," *J. Appl. Phys.*, vol. 43, p. 4190, 1972.
- [12] U. Nowak *et al.*, "The domain state model for exchange bias I: Theory," *Phys. Rev. B*, vol. 66, p. 014430-1, 2002.
- [13] Y.-T. Chen, "The effect of interface texture on exchange biasing in NiFe/IrMn system," *Nanoscale Res. Lett.*, vol. 4, p. 90, 2009.
- [14] Z. Y. Liu and S. Adenwalla, "Variation of domain formation in a 15 nm NiFe layer exchange coupled with NiO layers of different thicknesses," *Appl. Phys. Lett.*, vol. 82, p. 2106, 2003.
- [15] S. L. Moon-Hee Lee and K. Sin, "Enhanced exchange field of NiO/NiFe bilayer by dual ion beam sputtering process control," *Thin Solid Films*, vol. 320, pp. 298–304, 1998.
- [16] G. Li *et al.*, "Exchange bias effects of NiFe/NiO bilayers through ion-beam bombardment on the NiO surface," *Surface Coatings Technol.*, vol. 228, p. S437, 2013.
- [17] J. Nogues *et al.*, "Positive exchange bias in FeF₂-Fe bilayers," *Phys. Rev. Lett.*, vol. 76, p. 4624, 1996.